

**Serveur Académique Lausannois SERVAL [serval.unil.ch](http://serval.unil.ch)**

## **Author Manuscript**

**Faculty of Biology and Medicine Publication**

**This paper has been peer-reviewed but does not include the final publisher proof-corrections or journal pagination.**

Published in final edited form as:

**Title:** Isotropic Three-Dimensional T<sub>2</sub> Mapping of Knee Cartilage: Development and Validation

**Authors:** Colotti R, Omoumi P, Bonanno G, Ledoux JB, van Heeswijk RB

**Journal:** Journal of Magnetic Resonance Imaging

**Year:** 2017

**Volume:**

**Issue:**

**Pages:**

**DOI:** 10.1002/jmri.25755

# Isotropic Three-Dimensional T<sub>2</sub> Mapping of Knee Cartilage: Development and Validation

---

Roberto Colotti<sup>1</sup>, MSc, Patrick Omoumi<sup>1\*</sup>, MD, PhD, Gabriele Bonanno<sup>1,2,3</sup>, PhD, Jean-Baptiste Ledoux<sup>1,4</sup>, Ruud B. van Heeswijk<sup>1\*</sup>, PhD

**\* These authors contributed equally**

<sup>1</sup>Department of Radiology, University Hospital (CHUV) and University of Lausanne (UNIL), Lausanne, Switzerland

<sup>2</sup>Division of Cardiology, Department of Medicine, Johns Hopkins University, Baltimore, MD, USA

<sup>3</sup>Division of MR Research, Russell Morgan Department of Radiology and Radiological Sciences, Johns Hopkins University, Baltimore, MD, USA

<sup>4</sup>Centre for Biomedical Imaging (CIBM), Lausanne, Switzerland

**Address correspondence to:** Ruud B. van Heeswijk, PhD, Department of Radiology, Centre Hospitalier Universitaire Vaudois (CHUV), Rue de Bugnon 46, BH 08.084, 1011 Lausanne, Switzerland, email: ruud.mri@gmail.com

**Acknowledgments**

The authors would like to thank Prof. Matthias Stuber for fruitful discussions and the MR technologists of the CHUV for their extensive help with the MR scanning. This work has been supported by grants from the Pierre Mercier Foundation and the Swiss National Science Foundation (PZ00P3-154719) to RBvH, a R'Equip grant from the Swiss National Science Foundation (326030\_150828) to Prof. Matthias Stuber, as well as the Centre d'Imagerie BioMédicale (CIBM) of the UNIL, UNIGE, HUG, CHUV, EPFL, and the Leenaards and Jeantet Foundations.

**Running Title:** Isotropic 3D T<sub>2</sub> Mapping of Knee Cartilage

## **Abstract**

Purpose: I) To implement a higher resolution isotropic 3D  $T_2$  mapping technique that uses sequential  $T_2$ -prepared segmented gradient-recalled echo (Iso3DGRE) images for knee cartilage evaluation, and II) to validate it both in vitro and in vivo in healthy volunteers and patients with knee osteoarthritis.

Materials and Methods: The Iso3DGRE sequence with an isotropic 0.6mm spatial resolution was developed on a clinical 3T MR. Numerical simulations were performed to optimize the pulse sequence parameters. A phantom study was performed to validate the  $T_2$  estimation accuracy. The repeatability of the sequence was assessed in healthy volunteers (n=7).  $T_2$  values were compared to those from a clinical standard two-dimensional multi-slice multi-echo (MSME)  $T_2$  mapping sequence in knees of healthy volunteers (n=13) and in patients with knee osteoarthritis (OA, n=5).

Results: The numerical simulations resulted in 100 excitations per segment and an optimal RF excitation angle of  $15^\circ$ . The phantom study demonstrated a good correlation of the technique with the reference standard (slope  $0.9 \pm 0.05$ , intercept  $0.2 \pm 1.7$ ms,  $R^2 \geq 0.99$ ). Repeated measurements of cartilage  $T_2$  values in healthy volunteers showed a coefficient of variation of 5.6%. Both Iso3DGRE and MSME techniques found significantly higher cartilage  $T_2$  values ( $P < 0.03$ ) in OA patients. Iso3DGRE precision was equal to that of the MSME  $T_2$  mapping in healthy volunteers, and significantly higher in OA ( $P = 0.01$ ).

Conclusion: This study successfully demonstrated that high-resolution isotropic 3D  $T_2$  mapping for knee cartilage characterization is feasible, accurate, repeatable and precise. The technique allows for multiplanar reformatting and thus  $T_2$  quantification in any plane of interest.

**Keywords:** T<sub>2</sub> mapping, Isotropic 3D, Knee Cartilage, 3 Tesla, Osteoarthritis

## Introduction

To date, no effective cure exists to slow down or stop the progression of osteoarthritis (OA), a condition characterized by progressive cartilage degeneration (1). Because cartilage has limited repair capacity, the early detection of any local damage that precedes permanent cartilage tissue loss is an important target for research. Compositional magnetic resonance imaging (MRI) techniques have the potential to reflect the biochemical and ultrastructural composition of cartilage and provide quantitative information at the early stages of OA (1-3). Among these compositional MRI sequences,  $T_2$  mapping is used most in the clinic (1).

The spin-spin or  $T_2$  relaxation time is a physiological tissue property that reflects the water and collagen content of the extracellular matrix, as well as the structure of the collagen network (1,4).  $T_2$  relaxometry has been validated as a valuable quantitative imaging biomarker of the early changes of cartilage ultrastructure, and as an outcome measure for the development of new therapeutic solutions and cartilage repair procedures (3,5). In addition, the  $T_2$  relaxation time increases with the severity of OA and it can thus be also exploited for the grading of cartilage degeneration (6).

Most commonly used  $T_2$  mapping techniques are based on 2D pulse sequences with a limited number of slices and/or low through-plane resolution. The complex 3D anatomy of cartilage surfaces of the knee motivates the need for high-resolution 3D acquisitions that provide information on the entire joint without being subject to partial volume effects. In voxels that contain multiple tissues such as cartilage and fat, these partial volume effects mix their relaxation times, which may result in  $T_2$  measurement errors. Although 3D  $T_2$  mapping techniques have been previously developed to improve signal-to-noise ratio (SNR) and cartilage  $T_2$  quantification (7-11), there is still a need for a clinically

feasible submillimetric isotropic 3D  $T_2$  mapping technique that would allow I) reformats in an arbitrary plane II) minimization of partial volume effects, III) higher SNR per unit time compared to multiple 2D acquisitions, and IV) higher precision in  $T_2$  relaxation time quantification.

We therefore aimed to I) implement a high-resolution isotropic 3D  $T_2$  mapping technique that uses sequential  $T_2$ -prepared segmented gradient-recalled echo (Iso3DGRE) images for knee cartilage evaluation and to II) validate it both in vitro and in vivo in healthy volunteers and patients with knee OA.

## **Materials and Methods**

### Numerical simulations

Numerical simulations of the Bloch equations (12) were performed using Matlab (The Mathworks, Natick, MA) to find optimal pulse sequence parameters (number of excitations per segment ( $N_{ex}$ ) and radiofrequency (RF) excitation angle) that allowed for the maximum signal per unit time, while keeping the total scan duration as short as possible. Simulation parameters included relaxation times  $T_2=36.9\text{ms}$  and  $T_1=1240\text{ms}$  (similar to those of healthy cartilage (13)), a segmented k-space GRE acquisition with a centric readout order (14), a repetition time (TR) of 5.2ms, an echo time (TE) of 2.1ms, and incremental  $T_2$  preparation ( $T_{2prep}$ ) durations ( $TE_{T_{2prep}}$ ) of 0/23/38/53ms for variable  $T_2$  weighting (15,16). One dummy segment was simulated before the beginning of data acquisition in order to ensure a steady state condition.

## Acquisition protocol and $T_2$ fitting

We performed all MR experiments on a 3T clinical scanner (Magnetom Prisma, Siemens, Erlangen, Germany). A transmit/receive (Tx/Rx) 15-channel knee coil (Quality ElectroDynamics, Ohio, USA) was used. We implemented the Iso3DGRE pulse sequence (Figure 1) with the parameters detailed in Table 1. An adiabatic  $T_2$ prep (16) preceded the imaging part of the sequence. The minimum duration of the  $T_2$ prep module determined the second  $TE_{T_2prep}$  (i.e. 23ms). The excitation RF pulse was a 300 $\mu$ s sinc pulse with a bandwidth of 20.3kHz. A recovery time is used at the end of the acquisition to allow for longitudinal magnetization recovery and to decrease the specific absorption rate (SAR) load. The 4 input images were co-registered using 3D rigid registration (17,18) to account for subject motion during the acquisition. We performed pixel-wise  $T_2$ -mapping using the least-squares method in Matlab. The two-parameter fitting model used in this study is given by:

$$S(TE_{T_2prep}) = S_0 \cdot \left[ e^{\frac{-TE_{T_2prep}}{T_2}} + \frac{\delta}{T_2} \right], \quad (1)$$

where  $S_0$  is the initial signal when  $TE_{T_2prep}=0$ ms and  $\delta$  is an empirical offset (19). Given the long segmental acquisition time, the empirically determined  $T_2$ -fitting offset was added in order to correct for  $T_1$  recovery (15,20). We made this empirical offset sensitive to the  $T_2$  relaxation time for more accurate fitting.

## Phantom studies

We performed phantom studies to validate the results obtained from the simulations, to determine the fit offset  $\delta$  and then to test the in vitro accuracy in  $T_2$  determination of the

pulse sequence. Five phantoms were designed to approximate cartilage properties. They consisted of  $0.73\mu\text{M}$   $\text{NiCl}_2$  and varying concentration of agar (3 to 5% w/v) , and  $T_2$  maps were generated with the commercially available, clinical routine 2D multi-slice multi-echo spin echo (MSME) pulse sequence and the Iso3DGRE. In Iso3DGRE the  $\text{TE}_{T_2\text{prep}}$  series was similar to the TE series of MSME. Since echoes 2-6 in MSME pulse sequence contain a signal component from the stimulated echo, the  $T_2$  map was reconstructed by excluding the first echo (21). We used a 2D spin-echo (SE) sequence as a  $T_2$  reference standard, while we used an inversion-recovery spin-echo (IRSE) sequence to assure that the phantom  $T_1$  values were similar to those of human knee cartilage. A summary of the pulse sequence parameters is reported in Table 1.

We empirically chose the  $T_2$ -fitting offset such that the intercept value in the linear regression between the reference standard SE and the Iso3DGRE phantom  $T_2$  values was minimized. The optimal radiofrequency (RF) excitation angle of the Iso3DGRE  $T_2$  mapping pulse sequence was experimentally verified by imaging one of the agar phantoms (4% agar) with an RF excitation angle that was varied from  $5^\circ$  to  $30^\circ$ .

We approximated the relative SNR as the ratio between the signal in a region of interest (ROI) drawn in the phantom and the standard deviation of the noise in a ROI drawn well outside the phantom. In order to compare these experimental results to the numerical simulations, we normalized the maximal simulated signal to the maximal experimental relative SNR.

## Healthy volunteers

The institutional review board approved this cross-sectional study and we obtained written informed consent before each examination. The study group consisted of 13 healthy adult volunteers (eight men, body mass index (BMI)  $25.5 \pm 3.0 \text{ kg/m}^2$ , average age 33.2 years, range 27-39 years; five women, BMI  $21.1 \pm 2.2 \text{ kg/m}^2$ , average age 28 years, range 25-33 years). We selected all volunteers among a group of individuals that showed interest in participating in MR imaging research (i.e. a convenience sample) and did not have any history of knee trauma or surgery, pain or swelling. Minimal variation in cartilage loading before each scan was ensured.

We acquired an Iso3D GRE knee  $T_2$  map in all subjects with the readout in the head-foot direction. The image with  $TE_{T_2\text{prep}}=23\text{ms}$  was chosen for segmentation. ROIs were manually drawn (Matlab) by a research assistant (R.C., with 3 years of experience) under the supervision of a musculoskeletal radiologist (P.O., with 8 years of experience). We chose 15 continuous slices such that the central regions of the lateral and medial condyles were covered. The femoral and the tibial cartilage were segmented on these slices, after which eight cartilage compartments were defined on the sagittal plane (femoral lateral anterior, femoral lateral central, femoral lateral posterior, tibial lateral, femoral medial anterior, femoral medial central, femoral medial posterior and tibial medial). We used the anterior and posterior margins of, respectively, the anterior and posterior menisci to distinguish between the central and the anterior/posterior femoral compartment. Next, the average  $T_2$  value was calculated within each resulting ROI.

We also acquired a MSME  $T_2$  map (described above). We analyzed three slices in the central region of the lateral and medial condyles that covered the same volume analyzed for the Iso3DGRE  $T_2$  mapping, where the image of the first echo was used for segmentation. Similar to the Iso3DGRE technique, the femoral and the tibial cartilage were segmented and eight cartilage compartments were defined.

To test the repeatability in  $T_2$  values determination, the Iso3DGRE knee  $T_2$  map of seven healthy volunteers (four men, BMI  $26.2 \pm 3.5 \text{ kg/m}^2$ , average age 33.0 years, range 27-38 years; three women, BMI  $22.1 \pm 2.4 \text{ kg/m}^2$ , average age 28.7 years, range 25-33 years) was re-acquired 8 weeks after the first scan.

We performed relative SNR measurements in the lateral and medial femoral cartilage (anterior, central and posterior) layers for both  $T_2$  map techniques. In particular, the longest  $TE_{T_2\text{prep}}$  (i.e. 53ms) Iso3DGRE image and the longest TE (i.e. 78ms) MSME image were used.

#### Patients with knee osteoarthritis

The institutional review board approved this cross-sectional study and we obtained written informed consent before each examination. The study group consisted of five consecutive (i.e. selection bias did not affect the decision of which subjects to include) adult patients (one man, BMI  $28.1 \text{ kg/m}^2$ , age 83 years; four women, BMI  $25.9 \pm 3.9 \text{ kg/m}^2$ , average age 67.8 years, range 61-75 years) who were treated in our institution for knee OA. We included patients based on the analysis of postero-anterior weight-bearing radiographs, read by a musculoskeletal radiologist (P.O., with 8 years of experience). Each femorotibial compartment was graded separately using the Kellgren-Lawrence

criteria (22,23): grade 1= doubtful OA: doubtful narrowing of joint space and possible osteophytic lipping; grade 2= minimal OA: presence of definite osteophytes and possible joint space narrowing; grade 3= moderate OA: moderate multiple osteophytes, definite narrowing of joint space, some sclerosis and possible deformity of bone ends; grade 4= severe OA: presence of large osteophytes, marked narrowing of joint space, severe sclerosis and definite deformity of bone ends. We included patients with severe medial femorotibial OA (grade 4) and early lateral femorotibial OA (grade 1 (n=1) or 2 (n=4)). The OA grade on the patellofemoral compartment was not taken into account. Patients with history or imaging signs of previous knee surgery or traumatic ligamentous injury, rheumatologic or crystal arthropathy of the knee, and patients with contraindications to MRI were excluded. We acquired the Iso3DGRE and MSME knee  $T_2$  maps in all subjects with the same protocol as in the volunteer studies. ROIs were manually drawn on all cartilage surfaces with remaining cartilage and slices of interest were segmented as reported for the healthy volunteer studies.

We performed relative SNR measurements as in the volunteer studies.

### Statistical analysis

We conducted statistical analyses with GraphPad Prism 6.0 (GraphPad Software, Inc., La Jolla, CA), Matlab and computing environment R (R Development Core Team). The correlation and accuracy of both  $T_2$  mapping techniques and the reference standard SE were assessed with linear regression and Bland-Altman analysis (24). For each compartment, we analyze the distribution of the  $T_2$  values for each subject and for the femur and the tibia separately. We excluded extreme outlier  $T_2$  values that were beyond

cartilage  $T_2$  relaxation time physiological range from the analysis, since they were most likely the result of mis-registration (25) or partial volume effect; a  $T_2$  value was considered to be an extreme outlier if its distance to the interquartile interval of the ROI exceeds three times the length of this interval. Next, we calculated the mean  $T_2$  value and standard deviation of each compartment for both the patient and volunteer groups. A two-tailed Student's t-test was performed together with a Bland-Altman analysis in order to evaluate the difference in  $T_2$  values between patient and volunteers and between the Iso3DGRE and the MSME techniques, respectively. For in vitro and in vivo studies, we calculated the inverse of the precision of each technique as the ratio of the standard deviation and the average  $T_2$  value within the regions of interest (i.e. relative standard deviation). Finally, the repeatability of the  $T_2$  mapping was determined using the coefficient of variation (CoV), the intraclass correlation coefficient (ICC) (26) and the Bland-Altman analysis. Statistical significance was defined as  $P < 0.05$ .

## Results

### Numerical simulations

The optimized sequence parameters included 100 excitations per segment (Figure 2a) and RF excitation angle =  $15^\circ$  (Figure 2b). The minimum segmental acquisition time ( $T_{\text{seg}}$ ) was determined at the scanner and resulted to be 700ms due to specific absorption rate (SAR) limits.

### Phantom studies

The  $T_2$  relaxation times ranged from  $25.96 \pm 1.03$ ms to  $49.36 \pm 1.59$ ms. The IRSE reference  $T_1$  relaxation time of all five phantoms was  $1340.4 \pm 15.0$ ms. In the phantom

studies (Figure 3a-c), Iso3DGRE  $T_2$  mapping slightly underestimated the SE  $T_2$  values (linear fit slope  $0.9\pm 0.05$ ) when the fit offset  $\delta$  was set to 3, while the MSME technique slightly overestimated them (linear fit slope  $1.05\pm 0.07$ ). Given the negligible linear fit intercept ( $0.2\pm 1.7$ ms), the relationship between the  $T_2$  values obtained with the SE and the Iso3DGRE technique was directly proportional, as opposed to that between the SE and MSME  $T_2$  values (linear fit intercept  $3.5\pm 2.6$ ms). A high goodness of fit of the linear regression between the SE and the Iso3DGRE  $T_2$  maps was observed ( $R^2=0.99$ ), while a similarly high goodness of fit ( $R^2=0.98$ ) was found between the SE and MSME  $T_2$  maps.

Averaged over all agar phantoms, the relative standard deviations were  $2.6\pm 0.4\%$  (Iso3DGRE) and  $3.1\pm 1.0\%$  (MSME,  $P=0.1$ ).

The Bland-Altman analysis resulted in a slightly smaller bias for the Iso3DGRE ( $-3.7$ ms,  $P=0.002$ , Figure 3d) than for the MSME technique ( $5.4$ ms,  $P<0.001$ , Figure 3e). Compared to the SE  $T_2$  values, the Iso3DGRE  $T_2$  values better agreed than those obtained with the MSME technique for smaller  $T_2$  values. A minor trend of underestimation was found in Iso3DGRE  $T_2$  values, as opposed to the overestimation trend produced by the MSME technique. The limits of agreement were the same for both techniques ( $\pm 2.3$ ms, Figure 3d-e). The optimal RF excitation angle ( $15^\circ$ ) was experimentally determined and was in accordance with the simulated one for all  $TE_{T_2\text{prep}}$  (Figure 2b).

### Healthy volunteers

In all the eight compartments and in accordance to what was observed in the phantom study, the Iso3DGRE  $T_2$  values were significantly lower than those determined with the

MSME technique ( $P < 0.001$  for all comparisons, Figure 4a-b, Table 2) and allowed for multiplanar reformatting (Figure 5). The Bland-Altman analysis resulted in a bias of  $-10.2\text{ms}$  ( $P < 0.001$ ) and limits of agreement of  $\pm 5.6\text{ms}$  (Figure 4c).

Averaged over all volunteers and compartments, the relative standard deviations were  $26.8 \pm 8.2\%$  (Iso3DGRE) and  $26.6 \pm 8.6\%$  (MSME,  $P = 0.81$ ).

The CoV varied from  $1.1\%$  for the femoral lateral central compartment to  $9.1\%$  for the tibial medial compartment, while the ICC varied from  $0.89$  for the femoral lateral central compartment to  $0.43$  for the femoral lateral anterior compartment (Table 3). The Bland-Altman analysis resulted in a bias of  $-0.70\text{ms}$  ( $P = 0.42$ ) and limits of agreement of  $\pm 4.5\text{ms}$ .

Averaged over all cartilage compartments and over all volunteers, the relative SNR was  $13.7 \pm 0.2$  for Iso3DGRE and  $48.7 \pm 4.4$  for MSME.

#### Patients with knee osteoarthritis

In the OA knees, the articular cartilage was missing in the tibial medial, femoral medial anterior and femoral medial central compartments (these compartments were not included in the analysis). In all the remaining compartments we found a significant difference ( $P < 0.03$  for all comparisons) between the  $T_2$  values obtained with the Iso3DGRE technique and the values obtained with the MSME  $T_2$  mapping technique, similarly to what we observed in the phantom and volunteer studies (Table 2). The Bland-Altman analysis resulted in a bias of  $-15.6\text{ms}$  ( $P < 0.003$ ) and limits of agreement of  $\pm 10.2\text{ms}$  (Figure 4d). Moreover, in each compartment, the average  $T_2$  values obtained with both the Iso3DGRE and the MSME sequences were higher in OA compared to healthy knees ( $P < 0.03$  and  $P < 0.02$  respectively for all comparisons), except for the

femoral lateral central compartment ( $P=0.38$  and  $P=0.82$  respectively). Averaged over all patients and compartments the relative standard deviations were significantly lower for the Iso3DGRE compared to the MSME sequence ( $23.0\pm 8.1\%$  vs.  $28.1\pm 8.6\%$  respectively,  $P=0.01$ ).

Averaged over all cartilage compartments and over all patients, the relative SNR was  $15.0\pm 1.1$  for Iso3DGRE and  $69.0\pm 0.2$  for MSME.

## Discussion

In this study we have developed and optimized a new isotropic 3D  $T_2$  mapping technique of knee cartilage. We validated our sequence through phantom studies that demonstrated a good correlation between  $T_2$  values obtained with the proposed technique and the SE reference standard. In vitro, the Bland-Altman analysis resulted in a smaller bias for the Iso3DGRE than for the MSME technique, indicating that the Iso3DGRE technique might have slightly higher accuracy in  $T_2$  determination, while the precision was the same for both techniques. However, the  $T_2$  values in the range of interest were slightly underestimated for Iso3DGRE, while for MSME the  $T_2$  values were overestimated, as established in several prior studies (27,28). Given the negligible intercept value that resulted from the linear regression between the SE reference standard and the Iso3DGRE-derived  $T_2$  values (0.2ms), this underestimation can potentially be corrected simply by using a scaling factor, if desired. In contrast, the standard MSME  $T_2$  mapping technique resulted in overestimated  $T_2$  values with equivalent (healthy volunteers) or even higher standard deviation (patients with OA) compared to those obtained with the proposed technique. An empirical offset might also be beneficial to improve the accuracy of the MSME pulse sequence, but this was

beyond the goal of the present study. The Iso3DGRE technique is thus characterized by higher precision in vivo, even if the acquired voxel volume was 4.5 times smaller than that of MSME. The difference in precision performance between the in vitro and in vivo studies might be caused by the lower motion sensitivity of Iso3DGRE due to the sequential acquisition and the source image co-registration. Conversely, the intrinsic acquisition strategy of the MSME pulse sequence removes the benefit of any potential image co-registration. Since each echo train acquires a line of each image, all images are subject to all motion that occurs, and the images do not have different motion states that can be corrected with respect to one another.

We furthermore validated the technique in both healthy volunteers and OA patients. In particular, we measured  $T_2$  values of preserved areas of cartilage in severely medial femorotibial osteoarthritic knees. These areas included the lateral femorotibial and the posterior medial femoral compartments. Previous studies, in fact, have shown that: I) the apparently preserved cartilage in unicompartmental OA shows histological and mechanical signs of early OA (29-31) and II) the posterior aspect of the femoral compartment affected by advanced stages of OA is preserved in up to 89%, while presenting hypertrophy, possibly due to swelling that occurs in early OA changes (32,33). Repeated cartilage  $T_2$  value measurements showed a small CoV (5.6%) and both the Iso3DGRE and MSME sequences demonstrated increased  $T_2$  values with OA in most compartments, as expected (4,6).

The main advantage of the Iso3DGRE technique is its high-resolution isotropic acquisition, which results in a voxel size that is about 3 times smaller ( $0.25\text{mm}^3$  vs.  $0.75\text{mm}^3$ ) than currently available  $T_2$  mapping sequences (28), and is comparable to the voxel size of routinely used 3D morphological sequences ( $\sim 0.125\text{mm}^3$ ). Several

morphological studies have shown that cartilage properties present great regional variations (32-37). Since this variability is assessed at high resolution, there is a need to correlate morphologic and compositional/biochemical data to better understand these changes, and the lack of sub-millimetric isotropic resolution of the latter has been a limiting factor so far.

At 10min, the acquisition time of the proposed isotropic 3D  $T_2$  mapping technique was slightly longer than that of clinical routine  $T_2$  mapping protocols, which usually take between 4 and 9min (7,8,11) . However, this increased acquisition time can be justified with the possibility of multi-planar reformatting: the isotropic data allows for the evaluation of the distribution of cartilage  $T_2$  values in any reformatted plane and thus the complete coverage of the articular surface. This might represent an improvement in knee cartilage imaging, since multiple time consuming 2D acquisitions in different planes are no longer necessary, partial volume effects in the slice direction are avoided, and  $T_2$  precision and accuracy are improved. Multiple 3D  $T_2$  mapping techniques for knee cartilage quantification have been developed, including double echo steady state (DESS) (7,8), triple echo steady state (TESS) (9) and spoiled gradient-echo (SPGR) (10,11). However, these studies mainly aimed at using a 3D approach to improve SNR and were limited by their anisotropic resolution, as a consequence of the trade-off between SNR and acquisition time. The average relative cartilage SNR for the in vivo studies was 15 in the longest  $TE_{T_2\text{prep}}$  image of the Iso3DGRE technique, and 59 in the longest TE image for MSME. This relative SNR represents just an approximation, since the setup made use of a phased array coil, and GRAPPA was enabled. As reported by Sandino et al. (38) an SNR of 15 in a 15-element RF coil should lead to a negligible

signal overestimation of ~5%, which might lead to a negligible  $T_2$  relaxation time overestimation of 3%.

The present study has several limitations. First, the number of analyzed subjects was relatively small. This might be responsible for the absence of significant difference, although expected (6), in the femoral lateral central cartilage Iso3DGRE  $T_2$  values between healthy subjects and patients with OA. Second, in order to keep the total acquisition time as short as possible, we did not use any fat signal suppression technique. Such a technique would allow for increased contrast at the subchondral bone-cartilage interface and suppression of chemical shift artifacts, but at the expense of longer acquisition time. However, McGibbon et al. (39) have demonstrated through cartilage thickness measurements that the effect of chemical shift artifacts (both phase-cancellation and misregistration) is not substantial with gradient echo sequences. In the present study, the effect of chemical shift was indeed minimal on the Iso3DGRE sequence compared to the MSME sequence. Third, the magic angle effect on the  $T_2$  map was not specifically investigated in this study. The use of  $T_2$  values averaged over compartments allowed the minimization of its bias. Fourth, we used the co-registration to only correct for rigid motion between acquisitions. Any motion during the acquisition or any residual non-rigid motion was not taken into account. However, given the rigid structure of the cartilage layer and the physical restraints we used to minimize knee mobility, we made the hypothesis that most subject motion was small and only translational. Fifth, our pulse sequence parameters were optimized separately due to the interplay between SAR limits, stimulation limits and parameter settings. Finally, neither the magnetization transfer nor the diffusion effects on  $T_2$  relaxation time quantification were quantified.

For future developments, by applying model-based compressed sensing (40) it should be possible to reduce the acquisition time or to improve the spatial resolution. The regularization effect intrinsic to the compressed sensing reconstruction would most likely result in more precise  $T_2$  relaxation times. Moreover, this potential time economy could be exploited to apply a time-consuming fat signal suppression technique (such as using spectrally selective RF pulses). Finally, the stability of the empirical offset used in this study when varying pulse sequence parameters should be investigated in a future study. In conclusion, we have developed, optimized and validated a new isotropic 3D  $T_2$  mapping technique of knee cartilage in phantoms, volunteers, and patients. This technique allows for isotropic acquisition, which is advantageous for the complex knee anatomy. Due to its reasonable acquisition time, this sequence could be used in larger cohorts of patients to provide valuable 3D quantitative data on cartilage and other structures involved in OA such as the menisci, in order to improve our understanding of the disease and test new therapeutic solutions.

## References

1. Link TM, Neumann J, Li X. Prestructural cartilage assessment using MRI. *J Magn Reson Imaging* 2016.
2. Roemer FW, Crema MD, Trattnig S, Guermazi A. Advances in imaging of osteoarthritis and cartilage. *Radiology* 2011;260(2):332-354.
3. Guermazi A, Crema MD, Roemer FW. Compositional Magnetic Resonance Imaging Measures of Cartilage--Endpoints for Clinical Trials of Disease-modifying Osteoarthritis Drugs? *J Rheumatol* 2016;43(1):7-11.
4. David-Vaudey E, Ghosh S, Ries M, Majumdar S. T2 relaxation time measurements in osteoarthritis. *Magn Reson Imaging* 2004;22(5):673-682.
5. Guermazi A, Roemer FW, Alizai H, et al. State of the Art: MR Imaging after Knee Cartilage Repair Surgery. *Radiology* 2015;277(1):23-43.
6. Dunn TC, Lu Y, Jin H, Ries MD, Majumdar S. T2 relaxation time of cartilage at MR imaging: comparison with severity of knee osteoarthritis. *Radiology* 2004;232(2):592-598.
7. Welsch GH, Scheffler K, Mamisch TC, et al. Rapid estimation of cartilage T2 based on double echo at steady state (DESS) with 3 Tesla. *Magn Reson Med* 2009;62(2):544-549.
8. Staroswiecki E, Granlund KL, Alley MT, Gold GE, Hargreaves BA. Simultaneous estimation of T(2) and apparent diffusion coefficient in human articular cartilage in vivo with a modified three-dimensional double echo steady state (DESS) sequence at 3 T. *Magn Reson Med* 2012;67(4):1086-1096.
9. Heule R, Ganter C, Bieri O. Triple echo steady-state (TESS) relaxometry. *Magn Reson Med* 2014;71(1):230-237.
10. Bolbos RI, Zuo J, Banerjee S, et al. Relationship between trabecular bone structure and articular cartilage morphology and relaxation times in early OA of the knee joint using parallel MRI at 3 T. *Osteoarthritis Cartilage* 2008;16(10):1150-1159.
11. Pai A, Li X, Majumdar S. A comparative study at 3 T of sequence dependence of T2 quantitation in the knee. *Magn Reson Imaging* 2008;26(9):1215-1220.
12. Bloch F. Nuclear Induction. *Phys Rev* 1946;70:460-474.
13. Gold GE, Han E, Stainsby J, Wright G, Brittain J, Beaulieu C. Musculoskeletal MRI at 3.0 T: relaxation times and image contrast. *AJR Am J Roentgenol* 2004;183(2):343-351.
14. Bernstein MA, King KF, Zhou XJ. *Handbook of MRI pulse sequences*. Elsevier 2004.
15. van Heeswijk RB, Feliciano H, Bongard C, et al. Free-breathing 3 T magnetic resonance T2-mapping of the heart. *JACC Cardiovasc Imaging* 2012;5(12):1231-1239.
16. Nezafat R, Stuber M, Ouwerkerk R, Gharib AM, Desai MY, Pettigrew RI. B1-insensitive T2 preparation for improved coronary magnetic resonance angiography at 3 T. *Magn Reson Med* 2006;55(4):858-864.
17. Studholme C, Hill DL, Hawkes DJ. Automated 3-D registration of MR and CT images of the head. *Med Image Anal* 1996;1(2):163-175.
18. Bonanno G, Puy G, Wiaux Y, van Heeswijk RB, Piccini D, Stuber M. Self-navigation with compressed sensing for 2D translational motion correction in free-breathing coronary MRI: a feasibility study. *PLoS One* 2014;9(8):e105523.
19. van Heeswijk RB, Piccini D, Feliciano H, Hullin R, Schwitter J, Stuber M. Self-navigated isotropic three-dimensional cardiac T2 mapping. *Magn Reson Med* 2015;73(4):1549-1554.
20. Bano W, Feliciano H, Coristine AJ, Stuber M, van Heeswijk RB. On the accuracy and precision of cardiac magnetic resonance T2 mapping: A high-resolution radial study using adiabatic T2 preparation at 3 T. *Magn Reson Med* 2016.

21. Smith HE, Mosher TJ, Dardzinski BJ, et al. Spatial variation in cartilage T2 of the knee. *J Magn Reson Imaging* 2001;14(1):50-55.
22. Kellgren JH, Lawrence JS. Radiological assessment of osteo-arthrosis. *Ann Rheum Dis* 1957;16(4):494-502.
23. Schiphof D, Boers M, Bierma-Zeinstra SM. Differences in descriptions of Kellgren and Lawrence grades of knee osteoarthritis. *Ann Rheum Dis* 2008;67(7):1034-1036.
24. Bland JM, Altman DG. Statistical methods for assessing agreement between two methods of clinical measurement. *Lancet* 1986;1(8476):307-310.
25. Raya JG, Dietrich O, Horng A, Weber J, Reiser MF, Glaser C. T2 measurement in articular cartilage: impact of the fitting method on accuracy and precision at low SNR. *Magn Reson Med* 2010;63(1):181-193.
26. Shrout PE, Fleiss JL. Intraclass correlations: uses in assessing rater reliability. *Psychol Bull* 1979;86(2):420-428.
27. Maier CF, Tan SG, Hariharan H, Potter HG. T2 quantitation of articular cartilage at 1.5 T. *J Magn Reson Imaging* 2003;17(3):358-364.
28. Juras V, Bohndorf K, Heule R, et al. A comparison of multi-echo spin-echo and triple-echo steady-state T2 mapping for in vivo evaluation of articular cartilage. *Eur Radiol* 2016;26(6):1905-1912.
29. Obeid EM, Adams MA, Newman JH. Mechanical properties of articular cartilage in knees with unicompartmental osteoarthritis. *J Bone Joint Surg Br* 1994;76(2):315-319.
30. Bert JM, Leverone J. Histologic appearance of "pristine" articular cartilage in knees with unicompartmental osteoarthritis. *J Knee Surg* 2007;20(1):15-19.
31. Moen TC, Laskin W, Puri L. The lateral compartment in knees with isolated medial and patellofemoral osteoarthritis: a histologic analysis of articular cartilage. *J Arthroplasty* 2011;26(5):783-787.
32. Omoumi P, Michoux N, Roemer FW, Thienpont E, Vande Berg BC. Cartilage thickness at the posterior medial femoral condyle is increased in femorotibial knee osteoarthritis: a cross-sectional CT arthrography study (Part 2). *Osteoarthritis Cartilage* 2015;23(2):224-231.
33. Omoumi P, Michoux N, Thienpont E, Roemer FW, Vande Berg BC. Anatomical distribution of areas of preserved cartilage in advanced femorotibial osteoarthritis using CT arthrography (Part 1). *Osteoarthritis Cartilage* 2015;23(1):83-87.
34. Favre J, Erhart-Hledik JC, Blazek K, Fasel B, Gold GE, Andriacchi TP. Anatomically-standardized maps reveal distinct patterns of cartilage thickness with increasing severity of medial compartment knee osteoarthritis. *J Orthop Res* 2017.
35. Shiomi T, Nishii T, Nakata K, et al. Three-dimensional topographical variation of femoral cartilage T2 in healthy volunteer knees. *Skeletal Radiol* 2013;42(3):363-370.
36. Kaneko Y, Nozaki T, Yu H, et al. Normal T2 map profile of the entire femoral cartilage using an angle/layer-dependent approach. *J Magn Reson Imaging* 2015;42(6):1507-1516.
37. Wirth W, Maschek S, Eckstein F. Sex- and age-dependence of region- and layer-specific knee cartilage composition (spin-spin-relaxation time) in healthy reference subjects. *Ann Anat* 2017;210:1-8.
38. Sandino CM, Kellman P, Arai AE, Hansen MS, Xue H. Myocardial T2\* mapping: influence of noise on accuracy and precision. *J Cardiovasc Magn Reson* 2015;17(1):7.
39. McGibbon CA, Bencardino J, Palmer WE. Subchondral bone and cartilage thickness from MRI: effects of chemical-shift artifact. *MAGMA* 2003;16(1):1-9.
40. Huang C, Graff CG, Clarkson EW, Bilgin A, Altbach MI. T2 mapping from highly undersampled data by reconstruction of principal component coefficient maps using compressed sensing. *Magn Reson Med* 2012;67(5):1355-1366.

## Tables

**Table 1.** Pulse sequence parameters used for the parametric mapping techniques.

Sequence parameters	Iso3DGRE	2D MSME	2D SE	2D IRSE
Slices (-)	144	36	1	1
Slice spacing (mm)	-	0.3	-	-
Repetition time (ms)	5.2	1630	7000	7000
Echo times (ms)	2.1	13, 26, 39, 52, 65, 78	6.8, 15, 30, 60,120, 250, 400	6.8
T <sub>2</sub> preparation durations (ms)	0, 23, 38, 53	-	-	-
Inversion times (ms)	-	-	-	23, 50, 100, 250, 500,1000, 2000, 4000
Receiver bandwidth (Hz/px)	301	208	300	300
Phase partial Fourier (-)	-	5/8	-	-
Slice partial Fourier (-)	3/4	-	-	-
Matrix size (-)	272 × 280 × 144	320 × 224	192 × 92	192 × 92
Acquired voxel volume (mm <sup>3</sup> )	0.63 × 0.63 × 0.63	0.52 × 0.73 × 3	1.3 × 1.3 × 6	1.3 × 1.3 × 6
GRAPPA factor* (-)	2×	2×	-	-
Scan time (min)	10.1	7.2	75	85

Iso3DGRE isotropic three-dimensional T<sub>2</sub>-prepared segmented gradient-recalled echo; 2D MSME two-dimensional multi-slice multi-echo; 2D SE two-dimensional spin-echo; 2D IRSE two-dimensional inversion-recovery spin-echo; GRAPPA generalized autocalibrating partially parallel acquisitions.\* Indicates GRAPPA acceleration applied in the in-plane phase encoding direction (y).

**Table 2.** Average cartilage T<sub>2</sub> values in healthy volunteers and patients with advanced knee OA.

		Iso3DGRE T <sub>2</sub> values (ms)							
		FLA	FLC	FLP	TL	FMA	FMC	FMP	TM
Healthy									
volunteers		33.4±3.4*	34.2±4.1	34.1±2.4*	27.3±3.2*	38.3±4.5	36.0±4.7	34.3±2.5*	35.6±4.2
Advanced									
OA		37.8±2.7*	36.1±3.7	41.7±1.2*	31.2±2.5*	-	-	40.8±3.3*	-
patients									
		MSME T <sub>2</sub> values (ms)							
		FLA	FLC	FLP	TL	FMA	FMC	FMP	TM
Healthy									
volunteers		48.0±4.3*	45.1±8.7	45.8±4.2*	37.4±3.6*	50.6±8.2	41.5±4.4	43.1±1.7*	43.1±5.7
Advanced									
OA		60.6±12.4*	44.2±2.4	57.6±4.9*	46.8±11.0*	-	-	56.2±11.0*	-
patients									

FLA femoral lateral anterior; FLC femoral lateral central; FLP femoral lateral posterior; TL tibial lateral; FMA femoral medial anterior; FMC femoral medial central; FMP femoral medial posterior; TM tibial medial.

\* Indicates significant difference in values between groups of subjects, P<0.03.

**Table 3.** Coefficient of variation (CoV) and intraclass correlation coefficient (ICC) for repeated  $T_2$  value measurements in healthy volunteers.

Cartilage compartment	$T_2$ CoV (%)	ICC
Femoral lateral anterior	8.3	0.43
Femoral lateral central	1.1	0.89
Femoral lateral posterior	7.2	0.64
Tibial lateral	2.1	0.77
Femoral medial anterior	4.8	0.64
Femoral medial central	4.5	0.87
Femoral medial posterior	7.5	0.62
Tibial medial	9.1	0.49
All	5.6	-

The Bland-Altman analysis resulted in a bias of -0.70ms (P=0.42) and limits of agreement of  $\pm 4.5$  ms.

## Figure legends

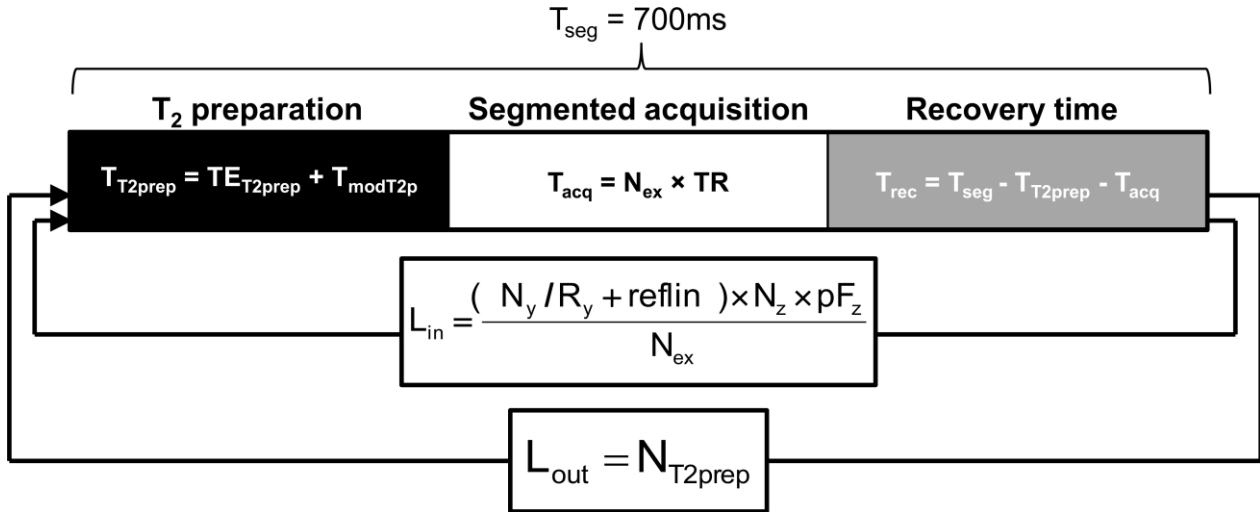


**Figure 1. Schematic representation of the Iso3DGRE pulse sequence.** The segment that is repeated in the inner loop to create one 3D image includes the  $T_2$  preparation module (in black), the segmented acquisition (in white) and the recovery time (in gray). The inner loop is repeated  $L_{\text{in}}$  times.  $T_{T2\text{prep}}$  is the total amount of time requested for the  $T_2$  preparation module and includes the echo time  $TE_{T2\text{prep}}$  as well as the true module duration  $T_{\text{mod}T2p}$  for playing out the other halves of the RF pulses and the spoiler gradient.  $T_{\text{acq}}$  indicates the total acquisition time per segment and is given by the repetition time (TR) multiplied with the number of excitations per segment  $N_{\text{ex}}$ . A recovery time ( $T_{\text{rec}}$ ) is used at the end of the acquisition to allow for longitudinal magnetization recovery and to decrease the specific absorption rate (SAR) load.  $T_{\text{rec}}$  is calculated by subtracting  $T_{T2\text{prep}}$  and  $T_{\text{acq}}$  from the total segmented acquisition time ( $T_{\text{seg}}$ ). The outer loop is repeated  $L_{\text{out}}$  times, which corresponds to the number of different  $T_2$  preparation times  $N_{T2\text{prep}}$ . At the end of each inner loop, a segment of a 3D k-space with a specific  $T_2$  weighting will have been acquired. At the end of each outer loop, a 3D dataset with different  $T_2$  weighting will have been acquired.  $N_y$  and  $N_z$

correspond to the numbers of phase encoding steps in the y and z directions, while pFz indicates the partial Fourier reconstruction factor in the z direction.  $R_y$  is the GRAPPA acceleration factor that is applied in the y direction with refline reference lines.

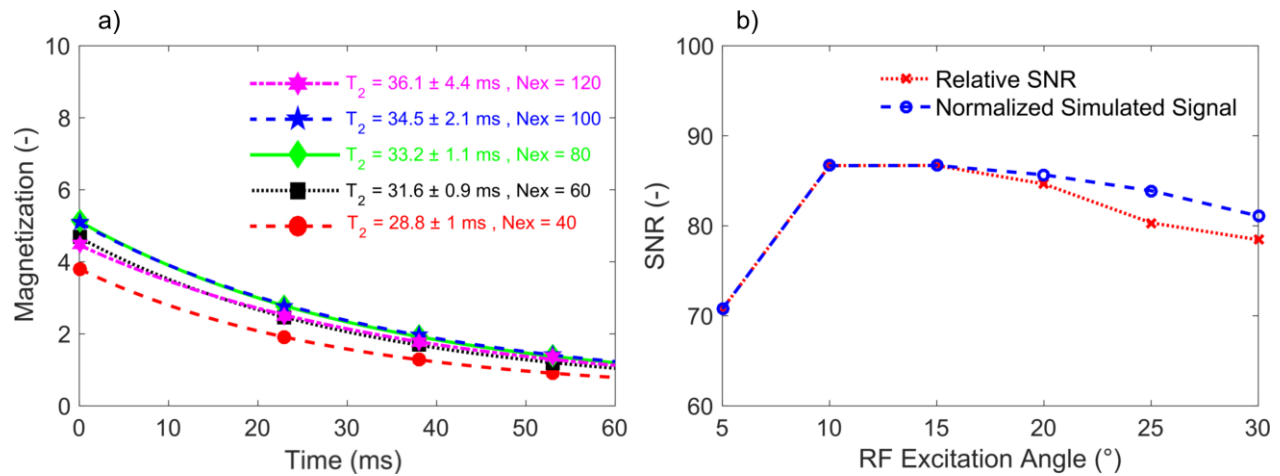


**Figure 2. Protocol optimization through Bloch equation simulations. a)** The magnetization as a function of time ( $TE_{T_2\text{prep}}$ ) for different number of excitations per segment ( $N_{ex}$ ). The minimum segmental acquisition time was 700ms due to specific absorption rate (SAR) constraints and the optimal  $N_{ex}$  that allowed to maximize the simulated magnetization was 100. **b)** The relative signal-to-noise ratio (SNR) in the phantom experiment and the normalized simulated signal as a function of the radiofrequency (RF) excitation angle for  $TE_{T_2\text{prep}}=23\text{ms}$  show a very similar curve shape, and resulted in an optimal RF excitation angle of  $15^\circ$ .

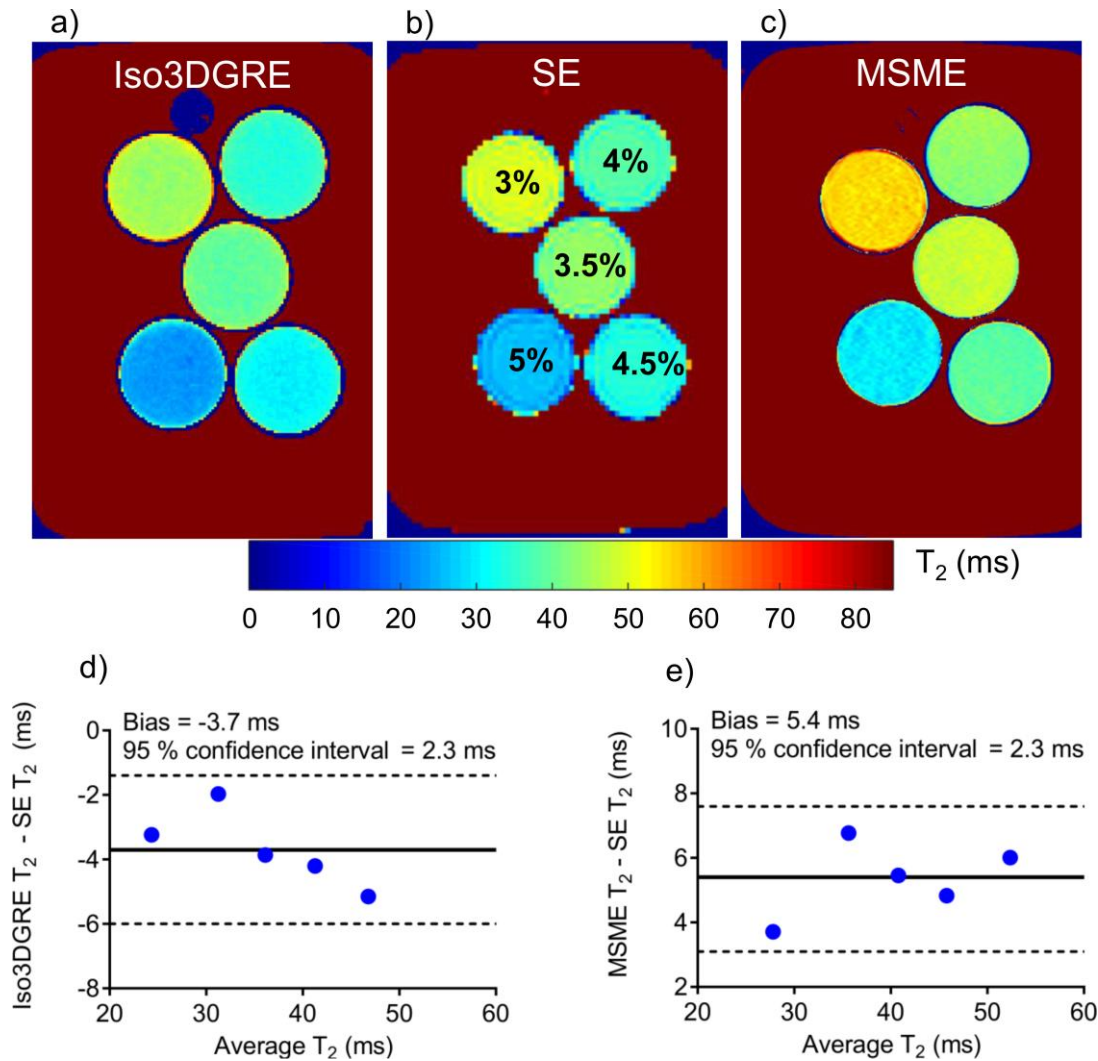


**Figure 3. In vitro comparison between three  $T_2$  mapping techniques.** **a)** An Iso3DGRE, **b)** an SE, and **c)** an MSME  $T_2$  map of five phantoms with similar  $T_1$  relaxation times and a range of  $T_2$  relaxation times as a function of agar concentration (3 to 5% weight/volume) that approximate those of cartilage. The percentage of agar is indicated in the middle map. SE  $T_2$  values range from  $26.0 \pm 1.0$  ms to  $49.4 \pm 1.6$  ms as a function of the agar concentration. Neither Iso3DGRE (difference up to -12%) nor MSME (difference up to 20%) agreed directly with SE for any phantom. **d)** The Iso3DGRE  $T_2$  mapping technique resulted in a bias of -3.7 ms ( $P=0.002$ ) and limits of agreement

of  $\pm 2.3$  ms. **e)** The MSME technique resulted in a bias of 5.4 ms ( $P < 0.001$ ) and limits of agreement of  $\pm 2.3$  ms. The dashed lines indicate the limits of agreement. A minor trend of underestimation in Iso3DGRE  $T_2$  values when compared to the SE-derived can be observed, as opposed to the overestimation trend produced by the MSME technique.

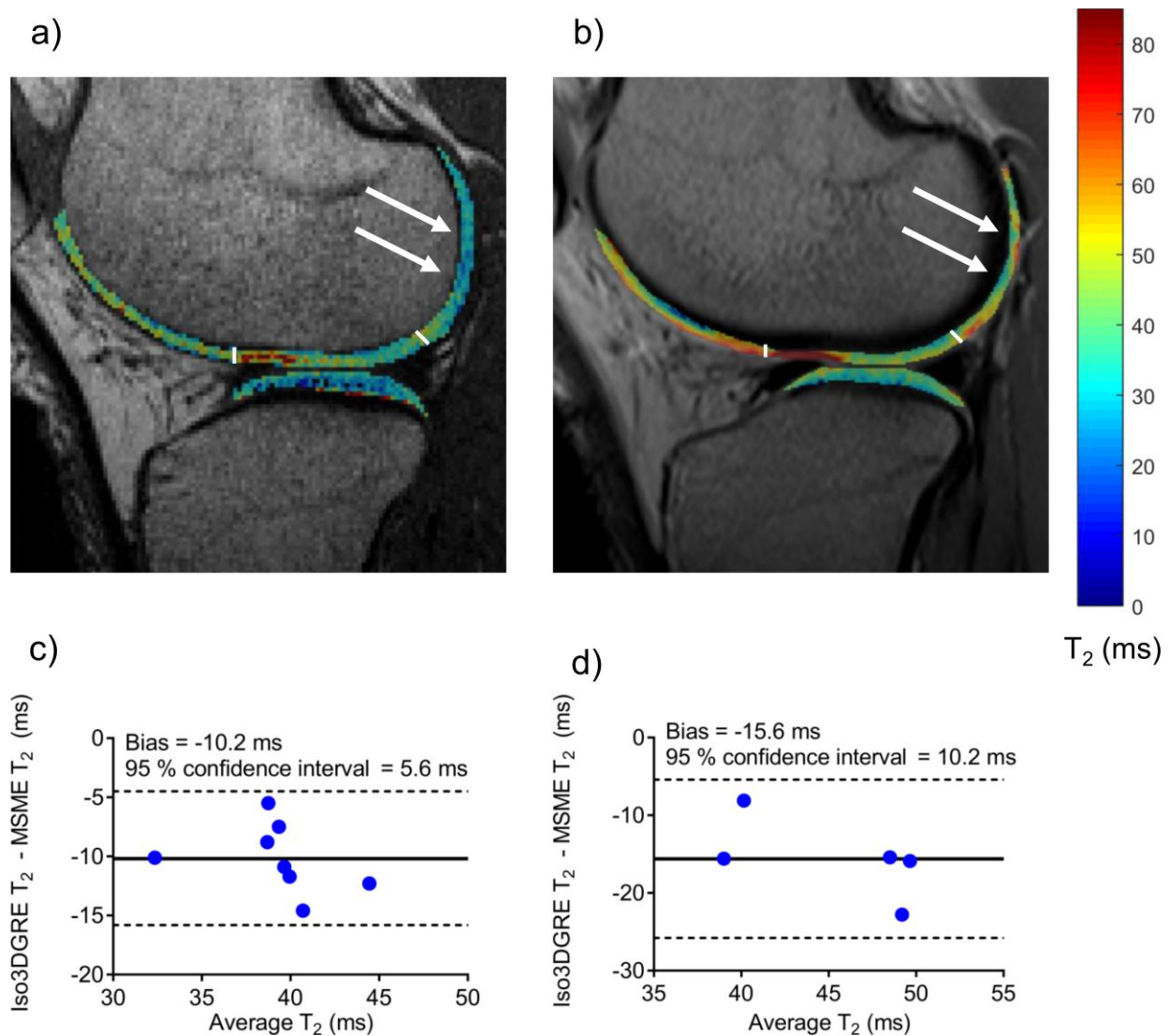


**Figure 4. Representative segmented  $T_2$  maps and in vivo comparison between two  $T_2$  mapping techniques. a) Iso3DGRE  $T_2$  map overlaid on related morphological image ( $TE_{T_2\text{prep}}=23$ ms) and b) MSME  $T_2$  map overlaid on related morphological image**

(TE=13ms). Femoral and tibial cartilage in both lateral and medial regions were manually segmented and then divided into 4 additional compartments (white divider lines). The Iso3DGRE  $T_2$  map is visually characterized by less pronounced chemical shift artifacts compared to the MSME  $T_2$  map (white arrows). **c)** A Bland-Altman analysis of the Iso3DGRE versus the MSME in the volunteer studies resulted in a bias of -10.2ms ( $P<0.001$ ) and limits of agreement of  $\pm 5.6$ ms. **d)** Similarly, the Bland-Altman analysis of the patient studies resulted in a bias of -15.6ms ( $P<0.003$ ) and limits of agreement of  $\pm 10.2$ ms. In both analyses, the Iso3DGRE  $T_2$  values were significantly lower than those determined with the MSME technique.

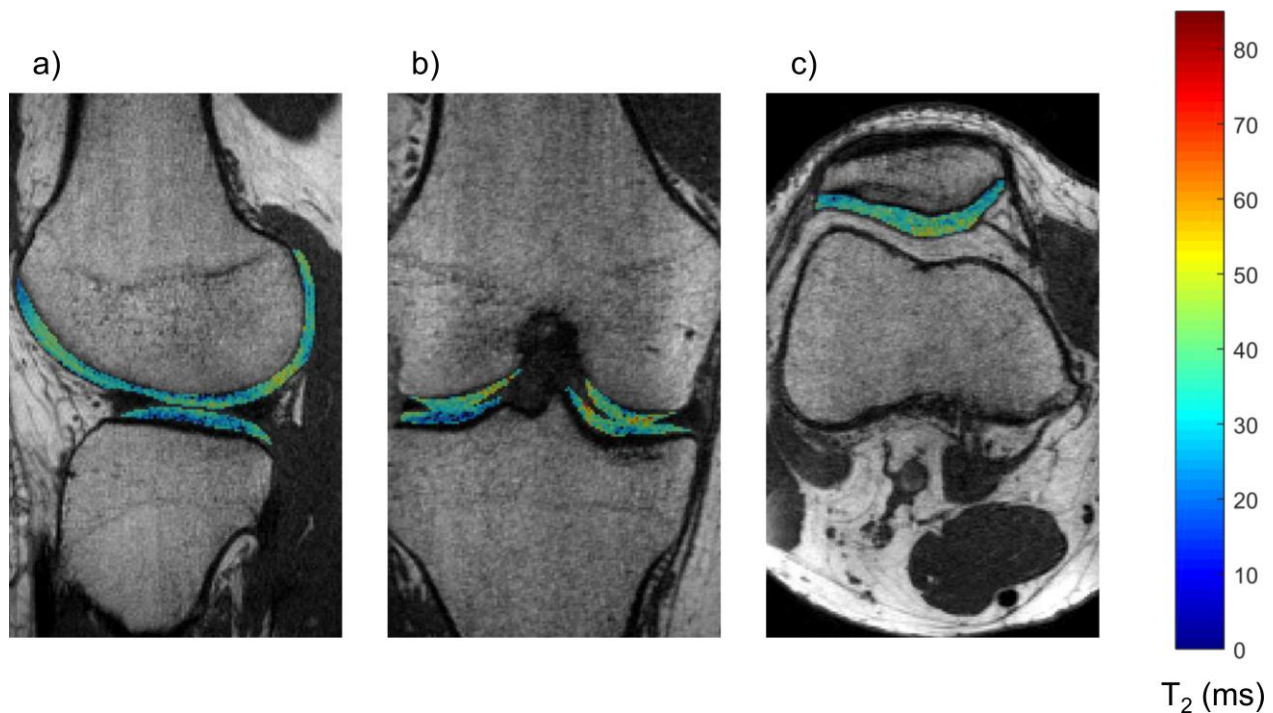


**Figure 5. A  $T_2$  map of a healthy volunteer acquired by Iso3DGRE overlaid on a morphological image. a)** Sagittal view of a knee for  $TE_{T_2\text{prep}}=23$ ms. The color-coded  $T_2$  map was overlaid. **b)** Reformatted coronal and **c)** axial view of the same volunteer on which the  $T_2$  map was overlaid. All views have identical pixel sizes.